Vol. 02, Iss. 1 (2025) 38-47, DOI: 10.61552/JSI.2025.01.005

Journal of Sustainable Development Innovations

www.jsi.aspur.rs

Stability Assessment of a Drivage in Jointed Rock Mass Using the Three Dimension Discrete Element Method

Sonu[a,*], Ashok Jaiswal[a], Varindra Saini[a]

[a]*Department of mining engineering, IIT-BHU, Varanasi, India.*

Keywords:

Drivage, 3DEC, Support Density, Failed Rock, Excavation.

* Corresponding author:

Sonu Saran

E-mail: sonu.rs.min18@itbhu.ac.in

Received: 12 July 2024
Revised: 19 August 2024
Accepted: 23 September 2024

A B S T R A C T

To run an underground mine effectively and safely, it is important to have a good understanding of the geotechnical behaviour around the underground excavations made in the mine. The stability of an underground drivage is influenced by many factors, primarily the in-situ stress, depth of drivage, orientation of discontinuities, intensity of jointing, groundwater, rock mass quality, shape and size of the drivage etc. This study is a continuation of stability analyses and support design of drivage, based on numerical methods. Generally rock bolt type support is used in underground excavation, to provide stability of the excavation. Using the information available on lithology, the orientation of discontinuities, in situ stress measurements, physical and mechanical properties of intact rock, discontinuities and, a three-dimensional numerical model was built by using the 3DEC software package to simulate a drivage excavation under in-situ stress condition. Numerical results have revealed that the total volume of failed blocks has reduced to 81.01%, 87.73%, 92.09%in case of 3 bolt support,4 bolt support,5 bolt support system with compare to no support system respectively. The greatest limitation in numerical modelling is the reliability of the input parameters. Hence, a parameter study on rock properties and field stress to be carried out properly.

1. INTRODUCTION

Tunnels are designed and constructed for Underground traffic, Water supply, and drainage, Excavation of minerals and fuel such as coal, iron, gold, etc., Military purposes like an underground fortification, Underground power plant, warehouse, Subways, and expressways [1].

In nature, most of the rock masses contain discontinuities. Such discontinuities include fissures, fractures, joints, faults, bedding planes, shear zones, and dikes. During, tunnel construction, rock discontinuities significantly affect the behavior of a rock mass around it. In underground excavations, discontinuities play a significant role in the deformation and stability of the rock mass around a tunnel [2].

Excavation of an underground tunnel in a mine can lead to deformation and stress redistribution. A good understanding of the geotechnical behavior through a stress analysis around a tunnel excavation helps one to design a proper support system and to ensure exploitation of the mine efficiently and safely [3]. In general, either the rock mass classification systems or discontinues or equivalent continuum method has been used to incorporate the influence of joints in rock mass mechanical behavior in evaluating the stability in underground excavations in jointed rock masses. Out of these three methods, discontinues stress analysis methods have the best capability of capturing the directional effects arising on deformability and stability from various orientations of discontinuity sets. [4, 5] Also, it has the capability of simulating large displacements and rotations that can occur with discontinuous rock masses [2, 6].

These following parameters to be responsible for the stability of underground excavations. (a) The height of rock cover; (b) span of the excavation; (c) intensity of jointing like the number of joint sets, mean spacing; (d) orientation of discontinuities; (e) shear strength of discontinuities; (f) strength of intact rock; and (g) groundwater conditions. The orientation of the discontinuities is critical to the failure modes of underground structures. The high in-situ stress is another unfavorable factor that may be encountered in underground problems. [7] It may cause large deformations and failure around the tunnels. Additionally, the configuration of the tunnel system, i.e., the distance between adjacent tunnels, heading directions of the tunnels, tunnel dimensions, also has great influences on the stability of surrounding rock masses [8].

For an underground mine, the development drifts are used to extract and transport the ore from the mining area. The safety of these tunnels plays essential roles in the economy and sustainability of the mine. Understanding the rock mass behavior around the tunnels is critical to select the supports, arrange the suitable construction sequences, and finally, help to avoid unnecessary disasters [9].

Supports is one of the most significant factors which should be considered during construction and long-term stability of the tunnel. There are two systems which applied to the support measurements of tunneling are rock reinforcement and rock support. Rock reinforcement is used to improve the strength and deformation behavior of the rock mass [7, 10] The reinforcement consists of steel bars such as bolts or cables which provides the additional strength to rock mass.

The primary objective of this study is to assess the Stability of the drivage in hard rock using discrete element method. The sub-objectives to meet the principal purpose are as follow:- (1) To quantify the effect of explicitly modeling the stress redistribution during the stand-up time between excavation and support (2) To assess the performance and adequacy of the support systems in the context of drivage stability (3) To maximum vertical displacement analysis concerning different roof bolt pattern and advancement.

2. NUMERICAL MODELING

The procedures adopted in modeling the tunnels are presented in this chapter. This begins with the process of creating a block, the boundary conditions, assigning in-situ stresses, joints and interface properties and discretization.

2.1 Model creation

The numerical model space is a polyhedron of dimensions 55 m along the tunnel length and a 55 m X 55 m square across the tunnel's cross-sectional profile. Note that the orientation of the coordinate system is presented at the bottom-left corner of Fig. 1. The tunnel axis (and maximum principal stress direction) is the z-axis, and the vertical axis is the y-axis. (G.F. Napa-garcia et.al, 2018) The minimum principal stress represents in the direction of the x axis. The orientation of the maximum principal stress is the actual spatial in the drivage/mine. Furthermore, the x-axis in the numerical model is set-up to go from x=-25 m to x=30 m, the y-axis ranges from y=-25 m to y=30 m, and the z axis ranges from z=-25 m to z=30 m and the centre of the block is x=2.5, y= 2.5, z= 2.5 [12].

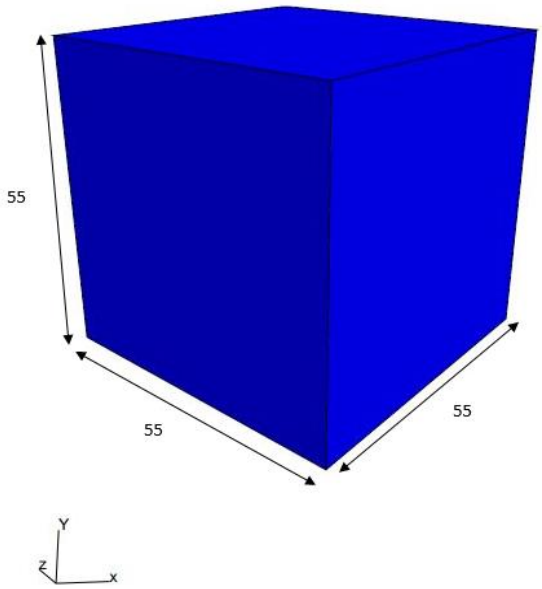

Fig. 1. Set-up numerical model with model dimension and without any joint.

To ensure that the model boundary is not influenced by the tunnel boundaries, the model dimensions have been carefully selected such that they are at least five times larger than the tunnel width in any direction from the tunnel. Three joint sets are introduced with their dip angles, dip directions and spacing in this model as shown in table 1. Fig. 3 shows the incorporated joint sets in 3 D block [13].

Table 1. Three joint sets with their orientation.

Sr.no.	Dip angle (in degree)	Dip direction (in degree)	Spacing (in m.)	No. of Joints
1	70	270	1.5	80
2	35	40	1.5	50
3	60	130	2.0	50

2.2 Stereo-net view of three joint sets

The trend characteristics of the joints (dip/dip direction) were measured by scanline method. In this study, we take three joint sets but in actual field case may be several numbers of joint sets present in the rock mass. These joint sets analyzed by DIPS software (RocScience,2010a) to get the dominant joint sets in the rock mass as shown in Fig. 2 [14].

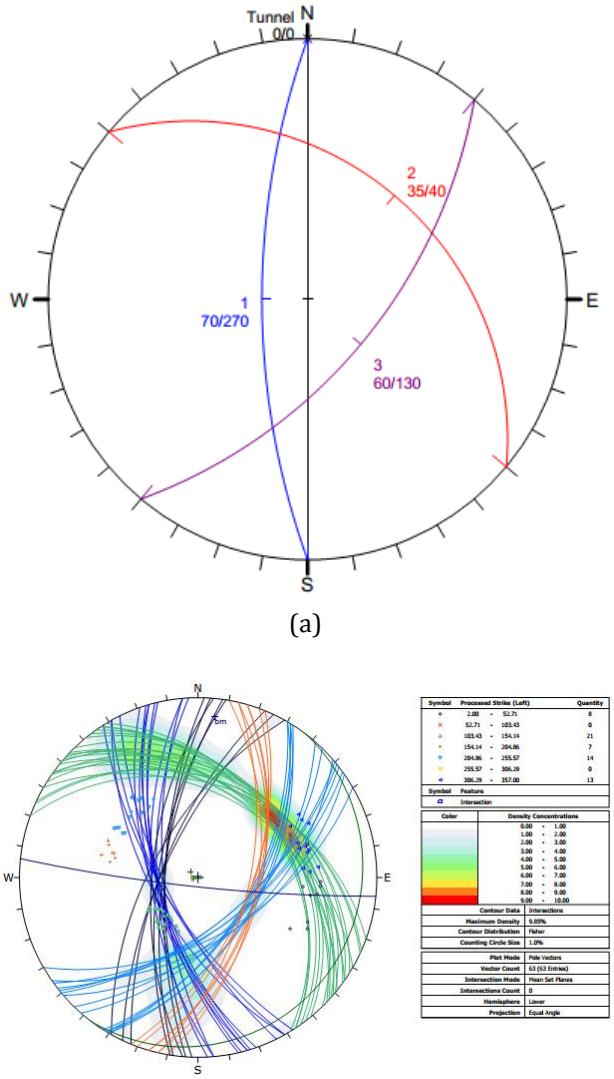

Fig. 2. (a) stereo-net view of three joint set with their dip and dip direction (b) intersection points view of these joint sets by dips software.

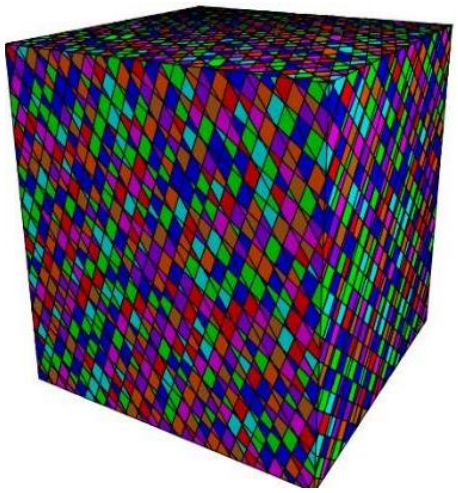

Fig. 3. Set-up 3-D block model with three joint sets.

2.3 Three Dimensional drivage Modelling

The in-situ stresses in the model have been assigned in each zone based on the vertical stress at 500 m, the stress gradient as dictated by gravity and the stress ratios. The boundary conditions in the model have been selected as a combination of stress and velocity constraints to ensure model stability and physical accuracy. The computational time increases with the number of discontinuities present in the model. To reduce the computational time, the length of the model in the z-direction is limited to 20 m as shown in fig 4. The physical and mechanical properties of the rock mass, joint(discontinuity) and bolt are in table 2, table 3 [14].

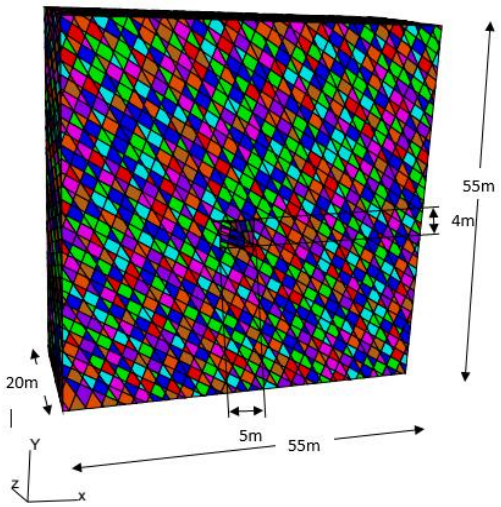

Fig. 4. A 3-D block model with dimensions of drivage

The model base has been fixed in the vertical direction, and vertical stress equal to overburden stress has been placed at y = 30 m (13.5 MPa). The four faces of the polyhedron have corresponding principal stresses and increasing stress gradients with depth. Fig. 5 shows the boundary conditions in the model in 2-dimensions

These three joint sets are assigned in this model with their dip angle and dip directions, which is measured by scale line method [15].

2.4 Material Properties

The physical and mechanical properties of rock and joints selected to represent lithology and to perform stress-deformation analysis are shown in Table 3 and table 4. The 3DEC has several built-in material behavior models.

Table 2. Mechanical property values of rock block in the numerical model.

Rock properties	Values
Young' modulus (GPa)	50
Poisson ratio	0.2
Density (kg/m^3)	2700
Stiffness (GPa/m)	27.778
Shear modulus (GPa)	20.833

Table 3. Mechanical property values of joints in the numerical model.

Joint set properties	Values
Friction angle (phi) (^{0})	28
Cohesion,C (MPa)	0
Tensile strength (MPa)	0
Normal stiffness JKn (GPa/m)	10
Shear stiffness JKs (GPa/m)	2

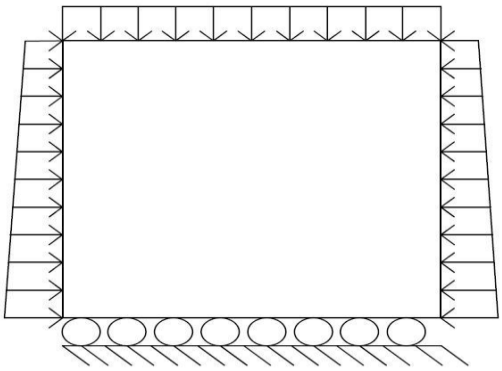

Fig. 5. Boundary conditions used in the numerical modelling.

2.5 Rock mass properties

There are different types of rocks in an area because of their different rock formation and their time duration. Thus, physical properties of rocks are varied in depth but in this study, we assume that rock has uniform properties.

For the Mohr-Coulomb plasticity model, the required properties are as : density, bulk modulus, shear modulus, friction angle, cohesion, dilation angle and tensile strength.

If any of these properties are not assigned, their values are set to zero by default. For both the elastic and Mohr-Coulomb models, density, bulk modulus, and shear modulus must be assigned positive values for *3DEC* to execute.

2.6 Triaxial test

Several specimens are tested at varying confining stresses to determine the shear strength parameters, the cohesion (c) and the angle of internal friction, moslty known as friction angle (φ). If data from several tests, carried out on different samples upto failure is available, then these results of the tests on each sample are plotted on a graph with the shear stress on the y-axis, and the normal confining stress on the x-axis and a series of Mohr circles can be plotted. It is convenient to show only the upper half of the Mohr circle. A line tangential to the Mohr circles can be drawn and is called the Mohr-Coulomb failure envelope as shown in fig 6. The y-intercept of the failure envelope which fits the test results is the cohesion, and the slope of the line or curve is the friction angle [9].

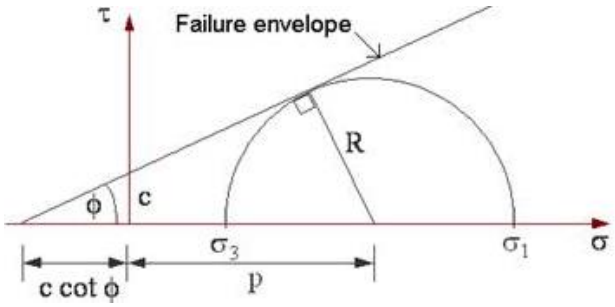

Fig. 6. The Mohr-Coulomb failure envelope.

The Mohr-Coulomb failure criterion can be written as the equation (1) for the line that represents the failure envelope. The general equation is

$$\tau = c + \sigma.\tan(\varphi) \quad (1)$$

Whereas:

τ = shear stress on the failure plane
c =cohesion
σ = normal stress on the failure plane
φ =angle of internal friction

The failure criterion can be expressed in terms of the relationship between the principal stresses. From the geometry of the Mohr circle [9],

$$\sin\phi = \frac{R}{c.\cot\phi + p} = \frac{\frac{\sigma_1 - \sigma_3}{2}}{c.\cot\phi + \frac{\sigma_1 + \sigma_3}{2}}$$

Rearranging,

$$\sigma_1 = \sigma_3\left(\frac{1+\sin\phi}{1-\sin\phi}\right) + 2c\sqrt{\frac{1+\sin\phi}{1-\sin\phi}} \quad (2)$$

whereas

$$\frac{1+\sin\phi}{1-\sin\phi} = \tan^2\left[\frac{\pi}{4} + \frac{\phi}{2}\right]$$

The Bulk modulus(*K*), and shear modulus (*G)*, are related to Young's modulus(*E)*, and Poisson's ratio(*ν)*, is given by the equation (3) and equation (4):

$$K = \frac{E}{3(1-2\nu)} \quad (3)$$

$$G = \frac{E}{2(1+\nu)} \quad (4)$$

2.7 In-situ stress

The underground geological Rock mass has a different kind of the stress depending on the overburden, geological structures, geological location and type of the rocks, etc. All kind of stress plays a significant role in the stability of the underground excavated structures. The weathering, irregular topography, residual stresses, erosion, and melting of the land ice are more influencing factors in the virgin state of the stress at shallow depth rather than greater depth. The ratio between horizontal and vertical stress is greater at greater depth rather than shallow [16].

The rock excavation at shallow depth may lead to more problems due to the presence of the horizontal or absence of the horizontal stress (Amadei and Stephansson, 1997). The stress in the rock can be considered as virgin and induced stress as a disturbance in the rock mass due to excavation. σv, σh, and σH are the virgin stress in the rock mass and can be considered by following relations [16].

$$\sigma_v = \rho.g.h \quad (5)$$

$$\sigma_H = k.\sigma_v = \frac{\nu}{1-\nu}\sigma v \quad (6)$$

2.8 Excavation sequence

Underground excavation in the rock mass is based on rock strength, i.e either rocks are soft or hard. If the rock formation is soft, generally Drilling and blasting method, TBM etc are used for excavation of rock but if the formation of the rock is hard, only drilling and blasting method is used for excavation of rock.

In the drilling and blasting method, excavation is done in a cyclic manner i.e. drilling-blasting-mucking and installation of adequate support. But support installation after each cycle of excavation is time consuming and at the same time, its increases the cost of operation. Thus, support installation might be done after two or more cycle of excavation. It will depend on the rock mass behaviour around the drivage or underground excavation.

Now a days, generally rock bolt type support is used in underground excavation, to provide stability of the excavation [17]. There are several different types of reinforcement considered to operate effectively in a range of ground conditions. One type is represented by a reinforcing bar or bolts fully encapsulated in a strong, stiff resin or grout. This system is considered by the comparatively large axial resistance to extensions that can be developed over a relatively short length of the shank of the rock bolt and by the high resistance to shear that can be developed by an element penetrating a sliping joint. The second type of reinforcement system, represented by cement-grouted cables or tendons, offers little resistance to joint shear, and development of full-axial load may require deformation of the grout over a substantial length of the reinforcing element. These two types of reinforcement are identified, respectively, as local reinforcement and global (or spatially-extensive) reinforcement. These two rock reinforcement systems have been incorporated into 3DEC. To support the excavation, here we use local reinforcement type (reinforcing bar or bolts fully encapsulated) support.

2.9 Support design

Various types of supports are installed to stabilize the underground excavation for long time use of this excavation as transport to men and material in the mining industry. Now a days, Rock bolt reinforcement is a most common support system in the mining indusrty. In this project work, we are using three different bolt patterns as a support system as shown in Fig 7.

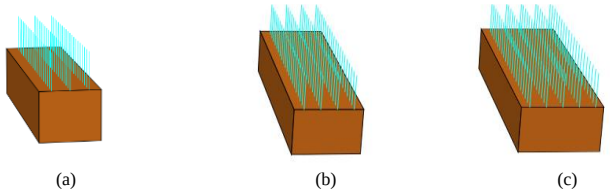

Fig. 7 (a) 3 Bolts support pattern with 1 m spacing (b) 4 Bolts support pattern with 1 m spacing (c) 5 Bolts support pattern with 1 m spacing.

2.10 Bolt properties

The local reinforcement elements used in *3DEC* require the following input parameters:

(1) axial stiffness [force/length]

(2) ultimate axial capacity [force]

(3) 1/2 active length [length]

(4) extensional failure strain (default = 10^{10})

(5) shear failure strain (default = 10^{10})

The value for 1/2 the active length can also be back-calculated from experimental testing.

The following theoretical expression may be used to estimate the axial stiffness, Ka, for fully-bonded solid reinforcing elements:

$$Ka = \pi \, k \, d_1 \qquad (7)$$

Where, $d1$ = reinforcement diameter

$$k = [\, 21 \, Gg \, E_b \, / \, (d_2 \, / \, d_1 - 1)] 1/2$$

The ultimate *axial* capacity of the reinforcement depends on a number of factors, including the strength of the reinforcing element, bond strength, hole roughness, grout strength, rock strength and hole diameter. In the absence of results of physical tests, empirical relations may be used to estimate the ultimate anchorage strength, P_{ult}. One such relation for the design of cement-grouted reinforcement is given by Littlejohn and Bruce (1975):

$$P_{ult} = 0.1 \, \sigma c \, \pi \, d_2 \, L \qquad (8)$$

Where, σc = uniaxial compressive strength of massive rocks (100% core recovery) up to a maximum value of 42 MPa, assuming that the compressive strength of the cement grout is equal to or greater than 42 MPa.

2.11 Probability of stability analysis

Analysis of drivage is based on the total volume of blocks which is falling or displacing beyond a certain limit with different support pattern and various bolt length. Initialy, calaculate the volume of displacing blocks around the drivage at without any support. Now, to design the support these three parameters are considered.

a) Bolt length (in m.)
b) Number of bolts per section
c) Excavation advancement (in m.)

Take all possible combination with the help of permutation, and combination theory. These all results are analysed according to failure percentage of rack mass.

Failure probability calculated by the probability formula which is given here;

$$\text{Probability} = \frac{\text{number of favorable outcomes}}{\text{number of possibl outcomes}}$$

The probability of an event always lies in the range of 0 to 1 (0% to 100%).

3. RESULT AND DISCUSSION

This study explores the stress relaxation and support stability quantification in terms of maximum displacement of blocks in the y-direction with and without support. The maximum velocity of blocks in the y-direction is also compared with different bolt support combinations.

3.1 Validating the input applied to the basic model

All the plots for this section are given on the plane perpendicular to the tunnel axis at z = 0. For each numerical analysis, it is important to check whether the unbalanced force reaches zero (whether the equilibrium has attained) before obtaining any plots. The distribution of xx-stress and yy-stress and the maximum compressive principal stress vector distributions are shown in fig. 8 [18].

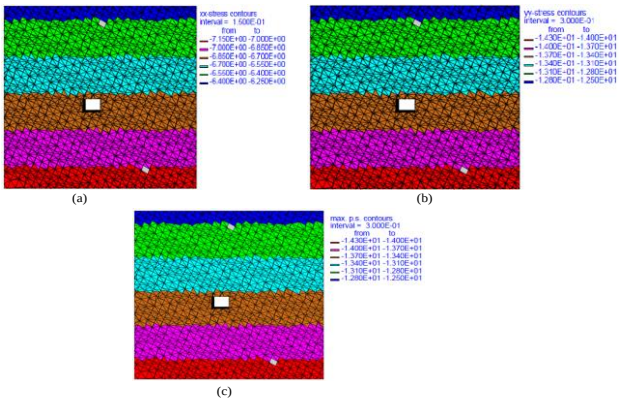

Fig. 8. (a) xx-stress distribution (in MPa) at zero steps, (b) yy-stress distribution (in MPa) at zero steps, (c) Maximum compressive principal stress vector distribution (in MPa) at zero steps.

3.2 Stress redistribution after excavation of drivage

When an opening is excavated in this rock, the stress field is locally disrupted, and a new set of stress is induced in the rock surrounding the opening. This is because rock, which previously contained stresses, has been removed and the load must be redistributed.

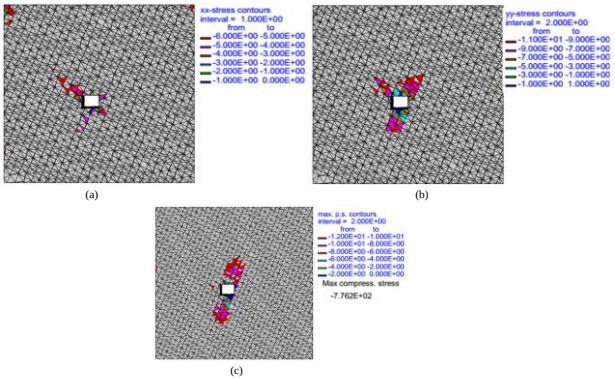

Fig. 9. Stress re-distribution after excavation (a) xx-stress (in MPa), (b) yy-stress (in MPa), (c) Maximum compressive principal stress vector (in MPa).

The re distribution of xx-stress and yy-stress and the maximum compressive principal stress vector distributions are shown in fig. 9, similar scenario is observed by [16].

3.3 Effect of rock support system on displacement around the drivage

Fig. 11 compares the X-displacement around the drivage for discontinuum analysis between without and with rock support systems. Fig. 12 compares the vertical displacement around the drivage for discontinuum analysis between without and with rock support systems. Both figures clearly show that the displacements have reduced by applying the rock support system. As clearly shown in fig. 10, Less number of blocks (in terms of volume) are falling with support system (3 bolts, 5 bolts) as compare to no rock support system at 30000 steps.

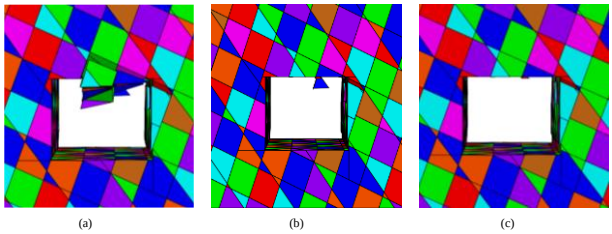

Fig. 10. View of blocks fall (a) without support at 30,000 steps, (b) three bolt support at 30,000 steps, (c) five bolt support at 30,000 steps.

The instability is also indicated by the vertical-displacement history plot in Figure 11 (a) With no support case and (b) with support at 30000 steps. In these histories, clearly shows that the maximum vertical displacement is being constant after a certain displacement in rock support condition but the maximum displacement is increasing continuously in no support condition. In other words, we can say blocks are stable after installation of rock support.

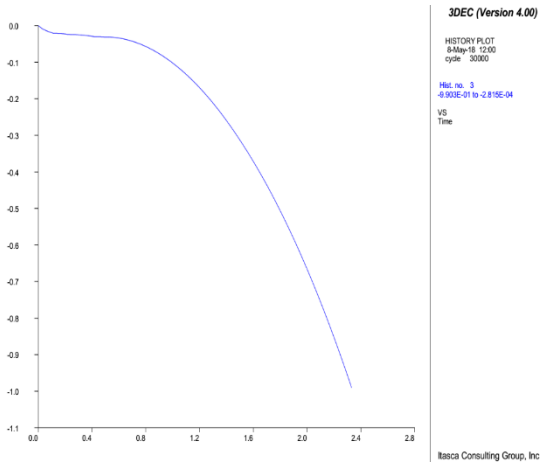

Fig. 11. (a) Graph between vertical displacement v/s time at without support.

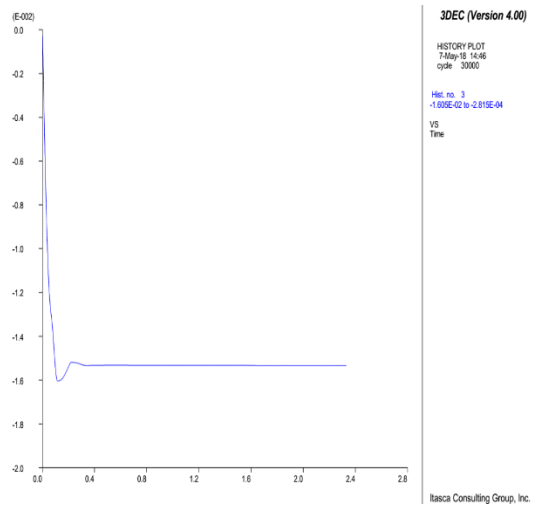

Fig. 11. (b) Graph between vertical displacement v/s time at with support.

Table 4. Comparison between different cases on total volume of roof fall (m^3) around the drivage.

Sr.no.	Support Yes/No	No. of bolts (in a row)	Bolt spacing (m.)	Total volume of roof fall (m^3)
1.	No	-	-	180.37
2.	Yes	3	1	34.25
3.	Yes	4	1	22.13
4.	Yes	5	1	14.26

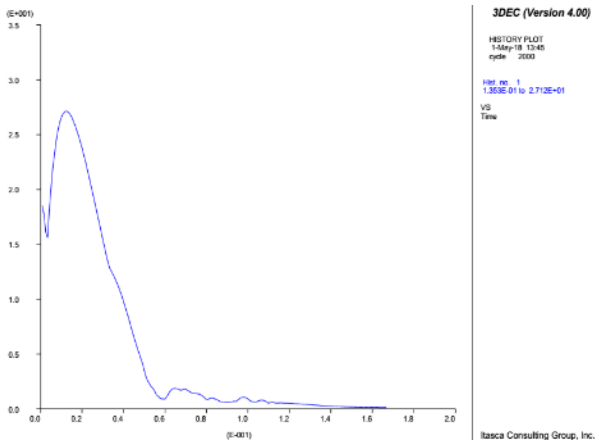

Fig 12 (a) Maximum unbalance force v/s time at without support.

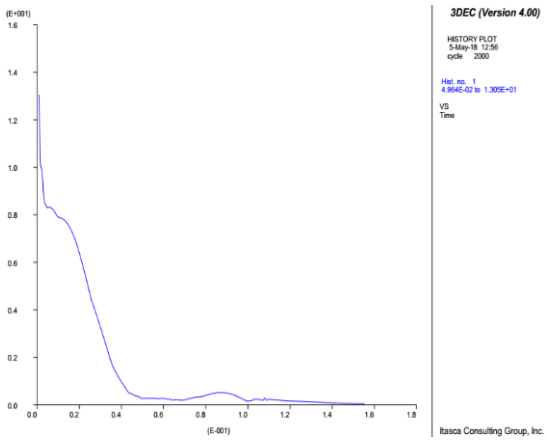

Fig. 12. (b) Maximum unbalance force v/s time at with support.

4. CONCLUSIONS

This study lays out numerical modeling studies performed on a rectangularly shaped drivage, driven in hard rock strata. Accurate 3-dimensional distinct element numerical models have been created using available data on the state of stress in the region and geological considerations, joint and intact rock properties drivage dimensions and support properties. The created numerical models have been tested and validated for correctness of applied input parameters. To establishes following analysis, with respect to various support system used to increase the stability of drivage in hard rock strata are as follow:

1) The relative total volume of roof fall (m^3) has reduced to 81.01% in case of 3 bolt support system with compare to no support system.
2) The relative total volume of roof fall (m^3) has reduced to 87.73% in case of 4 bolt support system with compare to no support system.

3) The relative total volume of roof fall (m^3) has reduced to 92.09% in case of 5 bolt support system with compare to no support system.

It has been found that the drivage undergo higher deformations and have larger fractured zones in the absence of supports and had the lowest overall deformation and size of fractured zones in the presence of supports in the roof. It has been found that the drivage undergo higher deformations and have larger fractured zones in the absence of supports and had the lowest overall deformation and size of fractured zones in the presence of supports in the roof.

Acknowledgement

The authors would like to express their gratitude to HOD of Department of mining engineering, Indian Institute of Technology (BHU), Varanasi, India for their kind support and providing computer lab. Facility.

REFERENCES

[1] H. Madkour, "Parametric analysis of tunnel behavior in jointed rock," *Ain Shams Engineering Journal*, vol. 3, no. 2, pp. 79–103, 2012, doi: 10.1016/j.asej.2012.01.002.

[2] Y. Xing and P. H. S. W. K. L. A. Sandbak, "Investigation of rock mass stability around tunnels in an underground mine by three-dimensional numerical modeling," pp. 579–597, 2017.

[3] Sonu and A. Jaiswal, "Time-Dependent Stability Assessment of Coal Mine's Gallery Using New Geotechnical Classification," *Journal of The Institution of Engineers (India): Series D*, vol. 105, no. 2, 2024, doi: 10.1007/s40033-024-00665-0.

[4] S. Fekete and M. Diederichs, "Integration of three-dimensional laser scanning with discontinuum modelling for stability analysis of tunnels in blocky rockmasses," *International Journal of Rock Mechanics and Mining Sciences*, vol. 57, pp. 11–23, Jan. 2013, doi: 10.1016/j.ijrmms.2012.08.003.

[5] Lisjak and G. Grasselli, "A review of discrete modeling techniques for fracturing processes in discontinuous rock masses," *Journal of Rock Mechanics and Geotechnical Engineering*, vol. 6, no. 4, pp. 301–314, 2014, doi: 10.1016/j.jrmge.2013.12.007.

[6] Y. M. Alshkane, A. M. Marshall, and L. R. Stace, "Prediction of strength and deformability of an interlocked blocky rock mass using UDEC," *Journal of Rock Mechanics and Geotechnical Engineering*, vol. 9, no. 3, pp. 531–542, 2017, doi: 10.1016/j.jrmge.2017.01.002.

[7] Sonu, S. Chawla, and A. Jaiswal, "An Experimental Study on Effect of Limited Boundness (LB) on Peak and Residual Strength of Intact Rock," *Min Metall Explor*, vol. 41, no. 2, 2024, doi: 10.1007/s42461-024-00963-x.

[8] S. Panthee, P. K. Singh, A. Kainthola, and T. N. Singh, "Control of rock joint parameters on deformation of tunnel opening," *Journal of Rock Mechanics and Geotechnical Engineering*, vol. 8, no. 4, pp. 489–498, 2016, doi: 10.1016/j.jrmge.2016.03.003.

[9] M. N. Bidgoli, Z. Zhao, and L. Jing, "Numerical evaluation of strength and deformability of fractured rocks," *Journal of Rock Mechanics and Geotechnical Engineering*, vol. 5, no. 6, pp. 419–430, 2013, doi: 10.1016/j.jrmge.2013.09.002.

[10] P. R. Gadepaka, Sonu, and A. Jaiswal, "Assessment of the strength deterioration of a coal pillar using a strain-softening time-dependent constitutive model," *Mech Time Depend Mater*, 2024, doi: 10.1007/s11043-024-09692-6.

[11] T. B. C. G. F. Napa-garcia, R. A. Sarantos, and A. T. Beck, "Improvement of analytical factor of saf...g failure mode in roof wedge stability.pdf," *International Journal of Rock Mechanics and Mining Science*, vol. 103, pp. 116–122, 2018.

[12] L. Bouzeran, J. Furtney, J. Hazzard, J. V. Lemos, and M. E. Pierce, "Simulation of ground support performance in highly fractured and bulked rock masses with advanced 3DEC bolt model," *Proceedings of the Eighth International Conference on Deep and High Stress Mining, Deep Mining 2017*, pp. 667–680, 2017.

[13] X. Wang, Y. Zhao, and X. Lin, "Determination of mechanical parameters for jointed rock masses," *Journal of Rock Mechanics and Geotechnical Engineering*, vol. 3, no. August, pp. 398–406, 2011, doi: 10.3724/SP.J.1235.2011.00398.

[14] A. Mohammadi and M. Hashemi, "Stability Analysis of Behesht-Abad Water Conveyance Tunnel Inlet Portal Using Experimental, Limit Equilibrium and Numerical Methods," 2013.

[15] H. Gumede and T. R. Stacey, "Measurement of typical joint characteristics in South African gold mines and the use of these characteristics in the prediction of rock falls," vol. 107, no. May, pp. 335–344, 2007.

[16] N. L. L. Mambou, J. Ndop, and J. M. B. Ndjaka, "Redistribution and magnitude of stresses around horse shoe and circular excavations opened in anisotropic rock," *International Journal of Mining Science and Technology*, vol. 25, no. 4, pp. 615–621, 2015, doi: 10.1016/j.ijmst.2015.05.015.

[17] M. Ø. Langåker, "Joberget tunnel - Analysis of stability and support design for tunneling in soil," no. June, 2014.

[18] P. H. S. W. K. Qiong Wu, "Application of equivalent continuum and...f a rock tunnel in a dam site in China.pdf," *Computers and Geotechnics*, vol. 46, pp. 48–68, 2012.

List of abbreviations

ρ = the density of the rock mass (kg/m3)

g = the gravity acceleration (m/s2)

h = the depth below ground surface (m)

σ_H = horizontal stress,

k = the stress ratio,

ν = Poisson's ratio, for most rock types ν value ranging from 0.15 to 0.35

G_g = grout shear modulus

E_b = Young's modulus of reinforcement material

d_1 = reinforcement diameter

d_2 = hole diameter.

σ_c = uniaxial compressive strength of massive rocks

L = bond length

K = Bulk modulus

G = Shear modulus

E = Young's modulus for rock